CRLB Performance for Widely Separated MIMO Radar in CES Disturbance

Neda Rojhani, Lorenzo Borghini, Maria S. Greco, Fulvio Gini
Department of Information Engineering, University of Pisa- Italy
Email: neda.rojhani@dii.unipi.it

***Abstract*—This paper addresses the problem of the target location and velocity estimation in Multiple-Input Multiple-Output (MIMO) radars with widely dispersed antennas. We derive the Cramér-Rao Lower Bounds (CRLB) on range and velocity of a target in the presence of Complex Elliptically Symmetric (CES) distributed clutter. Focusing on the particular case of Complex t-distribution clutter, we analyze the impact of the clutter spikyness on the estimation performance.**

***Index Terms*—Cramér-Rao lower bounds (CRLB), MIMO Radar, Joint Estimation, Complex Elliptically Symmetric (CES) distributed, Complex t-Distribution.**

I. Introduction

In recent years, Multiple-Input Multiple-Output (MIMO) radars have received a huge attention in radar literature. Many papers have been published [1], [2] regarding their performance for target detection [3], and target parameter estimation [4], considering both categories of MIMO systems, with widely separated antennas [4] and with closely spaced antennas [5].

Due to the remarkable characteristics of MIMO radars in estimating target parameters, various studies have been performed in different applications, including different antenna deployment [6], target models (motion or static target) [7], and various estimation algorithms [8], [9].

In this paper we derive the CRLBs on the estimation of target range and velocity with coherent MIMO radars in CES-distributed clutter. After the introduction of signal and clutter model, we focus on a specific CES distribution, the complex t-distribution that is often used in radar literature to model non-Gaussian spiky clutter [10], [11]. The CRLBs for the joint estimation of target range and velocity are derived and analyzed as function of clutter spikyness and Signal to Clutter power ratio (SCR).

II. Signal Model

Consider a coherent MIMO radar with M transmitter (TX) and N receiver (RX) antennas, widely dispersed in a 2-D plane as shown in Fig.1. In order to simplify the CRLB derivation we assume an isotropic target whose unknown complex amplitude is $\zeta = \zeta_R + j\zeta_I$. The unknown target location is (x, y) and the unknown target velocity is (v_x, v_y). The known locations of the M transmitters are $(x_k^t, y_k^t), (k = 1, ..., M)$ and of the N receivers are $(x_l^r, y_l^r), (l = 1, ..., N)$. Φ_k is the bearing of the kth transmitter, and ϕ_l is the bearing of the lth receiver with respect to the $x - axis$.

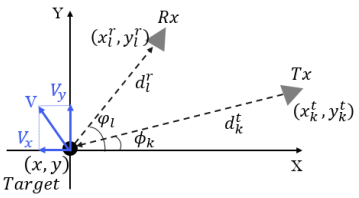

Fig. 1 Location of transmitters and receivers with respect to the moving target.

The echo of the lth receiver given from the transmission of all the M transmitters and reflected from the target, after down-conversion and sampling, is

$$r_l[n] = \sqrt{\frac{E}{M}}\zeta \sum_{k=1}^{M} e^{-j2\pi f_0 \tau_{lk}} e^{j2\pi f_{lk} n T_s} s_k(nT_s - \tau_{lk}) + z_l[n], \quad l = 1, ..., N \quad n = 1, ..., N_s \tag{1}$$

where ζ is the target complex reflectivity (deterministic and unknown), f_0 is the carrier frequency (carrier frequencies of all transmitters are assumed to be identical), T_s is the sampling time (chosen to satisfy the Nyquist criterion) and N_s is the number of samples in the observation period,$s_k(\Delta_n) = \mathrm{f}(\Delta_n) \cdot \mathrm{rect}(\frac{\Delta_n}{T_p})$ with $\Delta_n = (nT_s - \tau_{lk})$, is the complex baseband signal received by the lth receiver antenna sent by the kth transmitter antennas. The $\mathrm{rect}(\frac{\Delta_n}{T_p})$ part models the single pulse time interval while $\mathrm{f}(\Delta_n)$ refers to the specific class of signal implementation, and T_p refers to the pulse duration. Each signals is emitted by an individual transmitter antenna with energy E_s, while $E = E_s M$ is the total transmitted energy. Finally, $z_l[n]$ is the clutter echo at the lth receiver. τ_{lk} represents the time delay of a signal which propagates along the path from the kth TX antenna to the target, that is $d_k^t = \sqrt{(x_k^t - x)^2 + (y_k^t - y)^2}$, and then the path from the target to the lth RX antenna, that is $d_l^r = \sqrt{(x_l^r - x)^2 + (y_l^r - y)^2}$. Note that the $\tau_{lk} = \frac{d_k^t + d_l^r}{\lambda}$, where c is the speed of light. f_{lk} is the target Doppler frequency shift given by

$$f_{lk} = \frac{v_x(x_k^t - x) + v_y(y_k^t - y)}{\lambda d_k^t} + \frac{v_x(x_l^r - x) + v_y(y_l^r - y)}{\lambda d_l^r} \tag{2}$$

where λ is the wavelength of the carrier frequency.

In our derivation we assume that the transmitted signals are orthogonal. Furthermore, they retain approximately the

orthogonality, even after a variety of allowed time delays and Doppler frequency shifts, that is

$$\sum_{n=1}^{Ns} s_k(nT_s - \tau_{lk}) s_k^*(nT_s - \tau_{l'k'}) e^{j2\pi(f_{lk} - f_{l'k'})nT_s} \begin{cases} 1 & l = l', k = k' \\ 0 & l \neq l', k \neq k \end{cases} \quad \forall \tau_{lk}, f_{lk}, \tau_{l'k'}, f_{l'k'} \tag{3}$$

The N_s-dimensional observation vector at the lth receiver can be expressed as $\mathbf{r}_l = \{ \; r_l[1] \quad r_l[2] \quad ... \quad r_l[N_s] \; \}^T$. The observations from the set of all receivers can be written as the $N_s N$-dimensional vector $\mathbf{r} = \{ \; \mathbf{r}_1^T \quad \mathbf{r}_2^T \quad ... \quad \mathbf{r}_N^T \; \}^T$.

III. Complex elliptically symmetric distributions

Complex Elliptically Symmetric (CES) distributions are often used in cases where we need to model non-Gaussian heavy tailed radar clutter [12], [13]. The m-variate random vector (r.v) $z \in \mathbb{C}^m$, that follows the CES model has a probability density function (pdf) of the form

$$f_z(\mathbf{z}) = C_{m,g} \left|\Sigma\right|^{-1} g\Big((\mathbf{z} - \mu)^H \mathbf{\Sigma}^{-1} (\mathbf{z} - \mu)\Big) \tag{4}$$

where $\mu \in \mathbb{C}^m$ and $m \times m$ matrix $\mathbf{\Sigma}$ denote the mean vector and scatter matrix, respectively. The function g: $R_0^+ \rightarrow R^+$ the density generator, satisfies the constraint $\delta_{m,g} \triangleq \int_0^\infty t^{m-1} g(t) dt < \infty$, and $(.)^H$ refers the Hermitian (complex conjugate and transpose) operator. Lastly, $C_{m,g}$ is a normalizing constant such that $f_z(z)$ integrates to 1 and $C_{m,g} = 2(S_m \delta_{m,g})^{-1}$, where $S_m \triangleq \frac{2\pi^m}{\Gamma(m)}$. In short notation $z \sim CE_m(\mu, \mathbf{\Sigma}, g) = CE_{m,g}(\mu, \mathbf{\Sigma})$.

Therefore, the probability function of the received data vector $\mathbf{r}$ is

$$\mathbf{r} \sim CE_{N_s N, g}(\mu, \mathbf{\Sigma}) \tag{5}$$

where $\mu = \{ \; \mu_1^T \quad \mu_2^T \quad ... \quad \mu_N^T \; \}^T$, $\mu_l = \{ \; \mu_l[1] \quad \mu_l[2] \quad ... \quad \mu_l[N_s] \; \}^T$,$\mu_l[n] = \sqrt{\frac{E}{M}} \sum_{k=1}^M \zeta \Upsilon_{lk}[n] s_k(\Delta_n)$, and $\Upsilon_{lk}[n] = e^{-j2\pi f_0 \tau_{lk}} e^{j2\pi f_{lk} n T_s}$.

$\mathbf{\Sigma}$ is the space-time scatter matrix of the CES-distributed clutter.

IV. Cramér-Rao Lower Bound Expression

In this section, we derive the CRLBs for the MIMO radar. $\psi = [x, y, v_x, v_y, \zeta_R, \zeta_I]$ is the vector of all the unknown parameters in the received signal. Since we assume here that the target has already been detected and we now want to estimate target range and velocity, we consider the target reflectivity, ζ_R and ζ_I, as a nuisance parameter [14], [15], we derive the CRLBs of the unknown vector $\boldsymbol{\beta} = [x, y, v_x, v_y]$.

A. General CRLB for Location and Velocity Estimation

In order to derive the Cramér-Rao lower bounds of target location and velocity, the first step is to calculate the Fisher Information Matrix (FIM) and then to invert it, since the CRLB matrix is the inverse of the FIM $\mathbf{CRLB}(\psi) = [\mathbf{J}(\psi)]^{-1}$.

The FIM matrix is defined as

$$\mathbf{J}(\psi) = -E_{\mathbf{r},\psi}\Big\{ \frac{\partial}{\partial \psi} [\frac{\partial}{\partial \psi} \ln p(\mathbf{r}; \psi)]^T \Big\} \tag{6}$$

where $E\{.\}$ indicates the expectation operator and $\ln p(\mathbf{r}; \psi)$ is the Log-Likelihood (LL) function.

Since (1) is a function of time delay and Doppler frequency shift, we introduce the parameter vector as $\mathbf{\Theta} = [\tau_{11}, \tau_{12}, ..., \tau_{lk}, f_{11}, f_{12}, ..., f_{lk}, \zeta_R, \zeta_I]^T$, and, since ψ is a function of $\mathbf{\Theta}$, in order to compute the FIM, the chain rule [16] is applied , therefore, the FIM can be express as

$$\mathbf{J}(\psi) = \mathbf{P} \mathbf{J}(\mathbf{\Theta}) \mathbf{P}^T \tag{7}$$

where $\mathbf{P} = \frac{\partial \mathbf{\Theta}^T}{\partial \psi}$ depends on the geometry of the scenario and is given by

$$\mathbf{P} = \frac{\partial \mathbf{\Theta}^T}{\partial \psi} = \begin{bmatrix} \mathbf{U}_{4 \times 2NM} & \mathbf{0}_{4 \times 2} \\ \mathbf{0}_{2 \times 4} & \mathbf{I}_2 \end{bmatrix} \tag{8}$$

where $\mathbf{0}$ and $\mathbf{I}$ are the zero and identity matrix respectively, while $\mathbf{U}$ is given by

$$\mathbf{U} = \begin{bmatrix} \frac{\partial \tau_{11}}{\partial x} & ... & \frac{\partial \tau_{NM}}{\partial x} & \frac{\partial f_{11}}{\partial x} & ... & \frac{\partial f_{NM}}{\partial x} \\ \frac{\partial \tau_{11}}{\partial y} & ... & \frac{\partial \tau_{NM}}{\partial y} & \frac{\partial f_{11}}{\partial y} & ... & \frac{\partial f_{NM}}{\partial y} \\ 0 & ... & 0 & \frac{\partial f_{11}}{\partial v_x} & ... & \frac{\partial f_{NM}}{\partial v_x} \\ 0 & ... & 0 & \frac{\partial f_{11}}{\partial v_y} & ... & \frac{\partial f_{NM}}{\partial v_y} \end{bmatrix} \tag{9}$$

The details on the derivation of the elemements of $\mathbf{U}$ are in [16].

$\mathbf{J}(\mathbf{\Theta})$ is the Jacobian matrix given by

$$\mathbf{J}(\mathbf{\Theta}) = -E\Big\{ \frac{\partial}{\partial \mathbf{\Theta}} (\frac{\partial}{\partial \mathbf{\Theta}} \ln p(\mathbf{r}; \mathbf{\Theta}) \Big\} \tag{10}$$

where $p(\mathbf{r}; \mathbf{\Theta})$ is the pdf of the oberservation vector. In the derivation here, we consider the case of independent and identically distributed (i.i.d.) clutter samples in both time and space, then, if $r_l[n]$ is the generic sample of the observed signal of the lth receiver antenna,

$$p(r_l[n]; \mathbf{\Theta}) = \frac{1}{C_{1,g}} g(t_l[n]) \tag{11}$$

and the log-likelihood function is given by

$$\ln p(\mathbf{r}|\mathbf{\Theta}) = \ln \prod_{n=1}^{N_S} \prod_{l=1}^{N} p(r_l[n]|\mathbf{\Theta}) = C + \sum_{n=1}^{N_s} \sum_{l=1}^{N} \ln p(r_l[n]|\mathbf{\Theta}) = C + \sum_{n=1}^{N_s} \sum_{l=1}^{N} \ln g(t_l[n]) \tag{12}$$

where C is a generic constant that does not depend on the parameters of interest, $t_l[n]$ is the quadratic form $t_l[n] = \frac{1}{\sigma} \Big| r_l[n] - \sqrt{\frac{E}{M}} \zeta u_l[n] \Big|^2$, and $u_l[n] \triangleq \sum_{k=1}^{M} \Upsilon_{lk}[n] s_k[n]$.

A special case of CES-distributions is the Complex t-Distribution [17], in short notation $\mathbf{z} \sim Ct_{m,\nu}(\mu, \mathbf{\Sigma})$. In this case, the density generator is given by

$$g(t) = \left(1 + \frac{2t}{\nu}\right)^{\frac{-(2m+\nu)}{2}} \tag{13}$$

yielding $C_{m,g} = \frac{2^m \Gamma(\frac{2m+\nu}{2})}{(\pi\nu)^m \Gamma(\frac{\nu}{2})}$ as the normalizing constant. It is worth mentioning that ν denotes the shape parameter of the distrubution and it is related to the spikyness of the clutter. The lower the value of ν, the spikier is the clutter.

When the clutter is independent in both space and time domain the scatter matrix reduces to the scalar σ. In our derivations, if not differently specified, $\sigma = 1$. Each element of the Jacobian matrix is

$$\big[\mathbf{J}(\mathbf{\Theta})\big]_{i,j} = -E\Big[\frac{\partial^2 \ln p(\mathbf{r}|\mathbf{\Theta})}{\partial\Theta_i \partial\Theta_j}\Big] = -E\Big[\sum_{n=1}^{N_s}\sum_{l=1}^{N}\Big(\frac{g^{''}(t_l[n])}{g(t_l[n])} - \frac{g^{'}(t_l[n])^2}{g(t_l[n])^2}\Big)\frac{\partial t_l[n]}{\partial\Theta_i}\frac{\partial t_l[n]}{\partial\Theta_j} + \frac{g^{'}(t_l[n])}{g(t_l[n])}\frac{\partial^{'2} t_l[n]}{\partial\Theta_i\Theta_j}\Big] \quad i,j = 1,...,2NM+2 \tag{14}$$

It should be pointed out that, in calculating the second derivative of the LL function with respect to the parameters in (14) we should take into account the orthogonality assumption of the transmitted waveforms, which means that for instance, the derivative respect to the time delay $\frac{\partial^2 \ln p(\mathbf{r};\mathbf{\Theta})}{\partial\tau_{lk}\partial\tau_{l'k'}} = 0$ if $l \neq l^{'}, k \neq k^{'}$ because each signal given by each TX/RXelement is independent of the signal belonging to any other independent pair of TX/RX elements. Therefore if $l = l'$and $k = k'$, the generic element of (14) is achieved by considering the derivative expressions as follows

$$\frac{\partial t_p[n]}{\partial f_{lk}} = \Big(\frac{4\pi n T_s}{\sigma}\sqrt{\frac{E}{M}}\Im\Big\{\zeta\Upsilon_{lk}[n]s_k(\Delta_n)r_p^*[n]\Big\} - \frac{4\pi n T_s}{\sigma}\frac{E}{M}|\zeta|^2\Im\Big\{\Upsilon_{lk}[n]s_k(\Delta_n)u_p^*[n]\Big\}\Big)\delta(l-p) \tag{15}$$

$$\frac{\partial t_p[n]}{\partial \tau_{lk}} = \Big(-\frac{2}{\sigma}\sqrt{\frac{E}{M}}\Re\Big\{\zeta r_p^*[n]\Upsilon_{lk}[n]\Big(-j2\pi f_0 s_k(\Delta_n) + \dot{\mathrm{s}}_{\mathrm{k}}(\Delta_n)\Big)\Big\} + \frac{2}{\sigma}\frac{E}{M}|\zeta|^2\Re\Big\{u_p^*[n]\Upsilon_{lk}[n]\Big(-j2\pi f_0 s_k(\Delta_n) + \dot{\mathrm{s}}_{\mathrm{k}}(\Delta_n)\Big)\Big\}\Big)\delta(l-p) \tag{16}$$

$$\frac{\partial t_p[n]}{\partial \zeta_R} = -\frac{2}{\sigma}\sqrt{\frac{E}{M}}\Re\Big\{u_p[n]r_p^*[n]\Big\} + \frac{2}{\sigma}\frac{E}{M}\zeta_R\Big|u_p[n]\Big|^2 \tag{17}$$

$$\frac{\partial t_p[n]}{\partial \zeta_I} = \frac{2}{\sigma}\sqrt{\frac{E}{M}}\Im\Big\{u_p[n]r_p^*[n]\Big\} + \frac{2}{\sigma}\frac{E}{M}\zeta_I\Big|u_p[n]\Big|^2 \tag{18}$$

$$\frac{\partial^2 t_p[n]}{\partial\zeta_R\partial\zeta_R} = \frac{\partial^2 t_p[n]}{\partial\zeta_I\partial\zeta_I} = \frac{2}{\sigma}\frac{E}{M}\Big|u_p[n]\Big|^2, \qquad \frac{\partial^2 t_p[n]}{\partial\zeta_R\partial\zeta_I} = 0 \tag{19}$$

$$\frac{\partial^2 t_p[n]}{\partial f_{lk}\partial\zeta_R} = \Big(\frac{4\pi n T_s}{\sigma}\sqrt{\frac{E}{M}}\Im\Big\{\Upsilon_{lk}[n]s_k(\Delta_n)r_p^*[n]\Big\} - \frac{8\pi n T_s}{\sigma}\frac{E}{M}\zeta_R\Im\Big\{\Upsilon_{lk}[n]s_k(\Delta_n)u_p^*[n]\Big\}\Big)\delta(l-p) \tag{20}$$

$$\frac{\partial^2 t_p[n]}{\partial f_{lk}\partial\zeta_I} = \Big(\frac{4\pi n T_s}{\sigma}\sqrt{\frac{E}{M}}\Re\Big\{\Upsilon_{lk}[n]s_k(\Delta_n)r_p^*[n]\Big\} - \frac{8\pi n T_s}{\sigma}\frac{E}{M}\zeta_I\Im\Big\{\Upsilon_{lk}[n]s_k(\Delta_n)u_p^*[n]\Big\}\Big)\delta(l-p) \tag{21}$$

$$\frac{\partial^2 t_p[n]}{\partial\tau_{lk}\partial\zeta_R} = \Big(-\frac{2}{\sigma}\sqrt{\frac{E}{M}}\Re\Big\{r_p^*[n]\Upsilon_{lk}[n]\Big(-j2\pi f_0 s_k(\Delta_n) + \dot{\mathrm{s}}_{\mathrm{k}}(\Delta_n)\Big)\Big\} + \frac{4}{\sigma}\frac{E}{M}\zeta_R\Re\Big\{u_p^*[n]\Upsilon_{lk}[n]\Big(-j2\pi f_0 s_k(\Delta_n) + \dot{\mathrm{s}}_{\mathrm{k}}(\Delta_n)\Big)\Big\}\Big)\delta(l-p) \tag{22}$$

$$\frac{\partial^2 t_p[n]}{\partial\tau_{lk}\partial\zeta_I} = \Big(-\frac{2}{\sigma}\sqrt{\frac{E}{M}}\Re\Big\{jr_p^*[n]\Upsilon_{lk}[n]\Big(-j2\pi f_0 s_k(\Delta_n) + \dot{\mathrm{s}}_{\mathrm{k}}(\Delta_n)\Big)\Big\} + \frac{4}{\sigma}\frac{E}{M}\zeta_I\Re\Big\{u_p^*[n]\Upsilon_{lk}[n]\Big(-j2\pi f_0 s_k(\Delta_n) + \dot{\mathrm{s}}_{\mathrm{k}}(\Delta_n)\Big)\Big\}\Big)\delta(l-p) \tag{23}$$

$$\frac{\partial^2 t_p[n]}{\partial f_{lk}\partial f_{l'k'}} = \Big(\frac{8\pi^2 n^2 T_s^2}{\sigma}\sqrt{\frac{E}{M}}\Re\Big\{\zeta\Upsilon_{lk}[n]s_k(\Delta_n)\Big(r_p^*[n] - \sqrt{\frac{E}{M}}\zeta^* u_p^*[n]\Big)\Big\} + \frac{8\pi^2 n^2 T_s^2}{\sigma}\frac{E}{M}|\zeta|^2\Re\Big\{e^{-j2\pi f_0(\tau_{lk}-\tau_{l'k'})}e^{j2\pi(f_{lk}-f_{l'k'})nT_s}s_k(\Delta_n)s_k^*(\Delta_n)\Big\}\Big) \quad \delta(l-p,l-l',k-k') \tag{24}$$

$$\frac{\partial^2 t_p[n]}{\partial\tau_{lk}\partial\tau_{l'k'}} = \Big(-\frac{2}{\sigma}\sqrt{\frac{E}{M}}\Re\Big\{\zeta r_p^*[n]\Upsilon_{lk}[n]\Big(-4\pi^2 f_0^2 s_k(\Delta_n) - j4\pi f_0\dot{\mathrm{s}}_{\mathrm{k}}(\Delta_n) + \ddot{\mathrm{s}}_{\mathrm{k}}(\Delta_n)\Big)\Big\} + \frac{2}{\sigma}\frac{E}{M}|\zeta|^2\Re\Big\{\Upsilon_{lk}[n]u_p^*[n]\Big(-4\pi^2 f_0^2 s_k(\Delta_n) - j4\pi f_0\dot{\mathrm{s}}_{\mathrm{k}}(\Delta_n) + \ddot{\mathrm{s}}_{\mathrm{k}}(\Delta_n)\Big) + e^{-j2\pi f_0(\tau_{lk}-\tau_{l'k'})}e^{j2\pi(f_{lk}-f_{l'k'})nT_s}\Big(j2\pi f_0 s_k^*(\Delta_n) + \dot{\mathrm{s}}_{\mathrm{k}}^*(\Delta_n)\Big)\Big(-j2\pi f_0 s_k(\Delta_n) + \dot{\mathrm{s}}_{\mathrm{k}}(\Delta_n)\Big)\Big\}\Big) \quad \delta(l-p,l-l',k-k') \tag{25}$$

$$\frac{\partial^2 t_p[n]}{\partial f_{lk}\partial\tau_{l'k'}} = \Big(\frac{4\pi n T_s}{\sigma}\sqrt{\frac{E}{M}}\Im\Big\{\zeta r_p^*[n]\Upsilon_{lk}[n]\Big(-j2\pi f_0 s_k(\Delta_n) + \dot{\mathrm{s}}_{\mathrm{k}}(\Delta_n)\Big)\Big\} - \frac{4\pi n T_s}{\sigma}\frac{E}{M}|\zeta|^2\Im\Big\{u_p^*[n]\Upsilon_{lk}[n]\Big(-j2\pi f_0 s_k(\Delta_n) + \dot{\mathrm{s}}_{\mathrm{k}}(\Delta_n)\Big) + e^{-j2\pi f_0(\tau_{lk}-\tau_{l'k'})}e^{j2\pi(f_{lk}-f_{l'k'})nT_s}s_k(\Delta_n)\Big(j2\pi f_0 s_k^*(\Delta_n) + \dot{\mathrm{s}}_{\mathrm{k}}^*(\Delta_n)\Big)\Big\}\Big) \quad \delta(l-p,l-l',k-k') \tag{26}$$

Matrix $\mathbf{J}(\mathbf{\Theta})$, computed as in (14), can be divided into four sub-matrices as follows

$$\mathbf{J}(\mathbf{\Theta}) = \begin{bmatrix}\mathbf{D}_{2NM\times 2NM} & \mathbf{G}_{2NM\times 2} \\ \mathbf{G}^T_{2\times 2NM} & \mathbf{L}_{2\times 2}\end{bmatrix} \tag{27}$$

where $\mathbf{D} = \begin{bmatrix}\mathbf{D}_\tau & \mathbf{D}_{\tau f} \\ \mathbf{D}_{f\tau} & \mathbf{D}_f\end{bmatrix}$ in which $\mathbf{D}_\tau$, $\mathbf{D}_f$, and $\mathbf{D}_{\tau f} \in R^{NM\times NM}$. The lower right submatrix $\mathbf{L}$ involves derivatives of the target complex scattering coefficient, $\mathbf{L} = \begin{bmatrix}\mathbf{L}_{\zeta_R} & 0 \\ 0 & \mathbf{L}_{\zeta_I}\end{bmatrix}$. Finally, the upper right submatrix involves the derivatives related to all parameters: time delay, the Doppler frequency, and the target complex reflectivities, then $\mathbf{G} = \begin{bmatrix}\mathbf{G}_{\tau\zeta_R} & \mathbf{G}_{f\zeta_R} \\ \mathbf{G}_{\tau\zeta_I} & \mathbf{G}_{f\zeta_I}\end{bmatrix}$.

By exploiting the chain rule for (7), the FIM of ψ is given by

$$\mathbf{J}(\psi) = \begin{bmatrix}\mathbf{U}\mathbf{D}\mathbf{U}^T & \mathbf{U}\mathbf{G} \\ \mathbf{G}^T\mathbf{U}^T & \mathbf{L}\end{bmatrix} \tag{28}$$

Eventually, since our aim is to calculate the CLRBs of the vector β, we get

$$\mathbf{CRLB}_\beta = [\mathbf{U}(\mathbf{D} - \mathbf{G}\mathbf{L}^{-1}\mathbf{G}^T)\mathbf{U}^T)]^{-1} \tag{29}$$

where the diagonal elements of the CRLB matrix represent the lower bound of the variances of relevant parameters, hence: $CRLB_x = [CRLB_\beta]_{11}$, $CRLB_y = [CRLB_\beta]_{22}$, $CRLB_{vx} = [CRLB_\beta]_{33}$, and $CRLB_{vy} = [CRLB_\beta]_{44}$.

B. A Case Study

In this paragraph, the CRLBs are calculated for a simple MIMO radar system. Given the polar coordinates shown in Fig.2, a $M \times N = 4 \times 4$ MIMO radar is considered whose antenna bearings are $\big[\phi_1^t = \varphi_1^r = 0, \phi_2^t = \varphi_2^r = 90, \phi_3^t = \varphi_3^r = 180, \phi_4^t = \varphi_4^r = 270\big]$ with $d_k^t = d_l^r = 500\ m$ respectively. An isotropic target (T) with a complex scattering coefficient $\zeta = \frac{1+1j}{\sqrt{2}}$ is placed at $x = y = 0\ m$ with velocity $v_x = v_y = 10\ \frac{m}{s}$.

The carrier frequency is $f_0 = 10\ GHz$, the sample frequency is $f_S = 9\ MHz$, the pulse duration is $T_p = 0.56\ ms$,

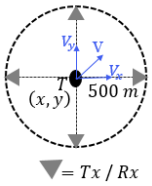

Fig. 2 Antenna placement

the observation time is $T_{obs} = 2.2\ ms$, and two different sets of waveforms are investigated; the first set is such that $\mathrm{f}(nT_s - \tau_{lk}) = \pm 1 \pm j$ in which the real and imaginary parts are randomly generated as $[-1,\ 1]$. In the second case, $\mathrm{f}(nT_s - \tau_{lk}) = e^{j2\pi n \Delta f (nT_s - \tau_{lk})}$ with frequency increment $\Delta f = 1\ MHz$ between $s_k[n]$ and $s_{k+1}[n]$ to satisfy the orthogonality assumption. Furthermore, each waveform has energy $E_s = 1$.

The Signal to Clutter power ratio (SCR) can be formulated as [18]

$$SCR = \frac{\sum_{k=1}^{M} \|s_k\|^2}{E\left\{z_l^H z_l\right\}} \tag{30}$$

Since the clutter is i.i.d. and t-distributed $E\left\{\mathbf{z}_l^H \mathbf{z}_l\right\} = N_s \frac{\nu}{\nu-2}\sigma$, where $E\left\{|z_l|^2\right\} = \frac{\nu}{\nu-2}\sigma$.

Fig.3 shows the relation of clutter power and the SCR as a function of the shape parameter ν for fixed energy of the signal and $\sigma = 1$.

Fig.4 shows the joint CRLBs of target location and velocity for different values ν for the second set of waveforms. It is worth noting that for $\nu = \infty$ the t-distribution concides with the Gaussian one. We only report $CRLB_x$, $CRLB_{vx}$, since we set the same numerical values for x and y as well as for v_x and v_y , therefore the CRLBs are the same.

In this figure, to obtain the CRLBs for varying ν, we fixed the signal power and we varied σ . From the figures it seems that, in this case, larger value of ν results in increasing the CRLBs, which leads to lower accuracy. Following this, we chose $\nu = 2.1$.

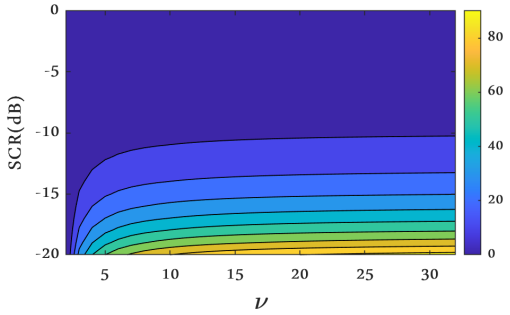

Fig. 3 Clutter Power vs degree of freedom and SCR

Fig.5 and Fig.6, demonstrate the CRLB results for the target location estimation and velocity estimation respectively, using random and exponential signals. With respect to Fig.5 and Fig.6, it is evident that the obtained CRLB is not particularly sensitive to the type of signal.

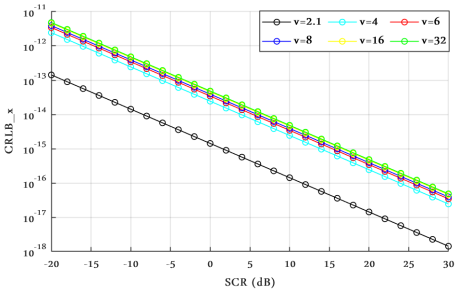

(a) Target location estimation

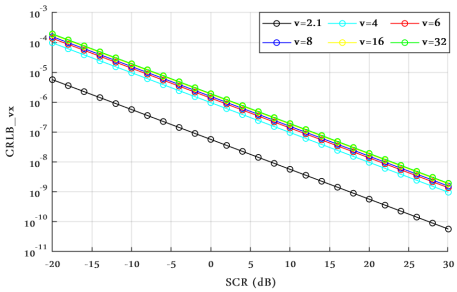

(b) Target velocity estimation

Fig. 4 CRLB estimation with different degree of freedom for Complex t-distribution

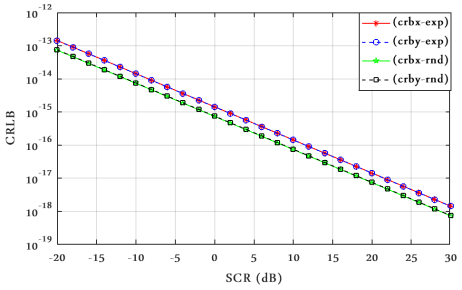

Fig. 5 CRLB comparison between the random (rnd) and exponential(exp) signals for target location estimation

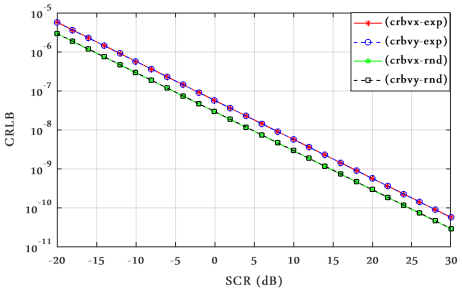

Fig. 6 CRLB comparison between the random (rnd) and exponential (exp) signals for target velocity estimation

Further, the analysis of the maximum achievable accuracy in parameter estimations (target and velocity) based on the target position can be show through the CRLBs. To extract the best accuracy (or the error) of target and velocity estimation we

can write

$$err_{xy} = \sqrt{CRLB_x + CRLB_y}$$
$$err_{vxvy} = \sqrt{CRLB_{vx} + CRLB_{vy}} \quad (31)$$

Fig.7 shows the maximum achievable accuracy gained by (31) in terms of CRLBs for both cases for varying positions and $v_x = v_y = 10$m/s. From these figures, we can observe that the accuracy around the up-right quadrant (the direction of the target's movement as $v_x > 0$ and $v_y > 0$) is lower. It is worth noting that the Doppler frequency is positive in the up-right quadrant, while it is negative in the opposite direction, as the object is moving away from lower antennas. These graphs are calculated for SCR$= -15\ dB$.

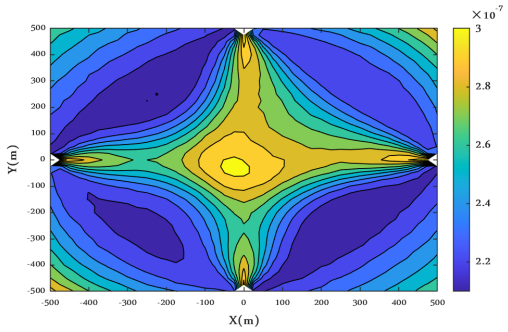

(a) Accuracy in Location Estimation

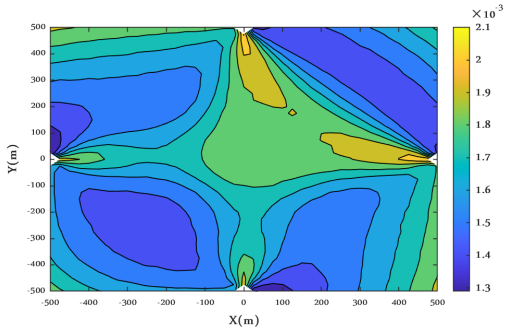

(b) Accuracy in Velocity Estimation

Fig. 7 Maximum achievable accuracy in position and velocity estimation when target is moving

V. Conclusion

This paper addresses the performance analysis of target position and velocity estimation in terms of CRLBs in widely separated MIMO radar in the presence of non-Gaussian CES-distributed clutter.

In particular, we derived the expressions of the CRLBs with orthogonally transmitted waveforms and white (in space and time) t-distributed clutter. We analyzed the CRLBs for two different set of waveforms as a function of the SCR and the spikiness of the clutter. The derivation of the CRLBs in presence of correlated (in space and/or in time) clutter is in order.

Acknowledgment

The work of M. Greco and F. Gini has been partially supported by the Italian Ministry of Education and Research (MIUR) in the framework of the CrossLab project (Departments of Excellence) of the University of Pisa, laboratory of Industrial Internet of Things (IIoT).

References

[1] E. Fishler, A. Haimovich, R. Blum, D. Chizhik, L. Cimini, and R. Valenzuela, "Mimo radar: An idea whose time has come," in *Proceedings of the 2004 IEEE Radar Conference (IEEE Cat. No. 04CH37509)*. IEEE, 2004, pp. 71–78. I

[2] J. Li and P. Stoica, *MIMO radar signal processing*. Wiley Online Library, 2009, vol. 7. I

[3] E. Fishler, A. Haimovich, R. S. Blum, L. J. Cimini, D. Chizhik, and R. A. Valenzuela, "Spatial diversity in radars—models and detection performance," *IEEE Transactions on signal processing*, vol. 54, no. 3, pp. 823–838, 2006. I

[4] A. M. Haimovich, R. S. Blum, and L. J. Cimini, "Mimo radar with widely separated antennas," *IEEE Signal Processing Magazine*, vol. 25, no. 1, pp. 116–129, 2007. I

[5] J. Li and P. Stoica, "Mimo radar with colocated antennas," *IEEE Signal Processing Magazine*, vol. 24, no. 5, pp. 106–114, 2007. I

[6] ——, "Concepts and applications of a mimo radar system with widely separated antennas," 2009. I

[7] A. Hassanien, S. A. Vorobyov, and A. B. Gershman, "Moving target parameters estimation in noncoherent mimo radar systems," *IEEE Transactions on Signal Processing*, vol. 60, no. 5, pp. 2354–2361, 2012. I

[8] P. Stoica and A. Nehorai, "Music, maximum likelihood, and cramer-rao bound: further results and comparisons," *IEEE Transactions on Acoustics, Speech, and Signal Processing*, vol. 38, no. 12, pp. 2140–2150, 1990. I

[9] M. Jiang, R. Niu, and R. S. Blum, "Bayesian target location and velocity estimation for multiple-input multiple-output radar," *IET radar, sonar & navigation*, vol. 5, no. 6, pp. 666–670, 2011. I

[10] F. Gini, "A radar application of a modified cramer-rao bound: parameter estimation in non-gaussian clutter," *IEEE transactions on signal processing*, vol. 46, no. 7, pp. 1945–1953, 1998. I

[11] K. J. Sangston, F. Gini, and M. S. Greco, "Coherent radar target detection in heavy-tailed compound-gaussian clutter," *IEEE Transactions on Aerospace and Electronic Systems*, vol. 48, no. 1, pp. 64–77, 2012. I

[12] S. Fortunati, F. Gini, M. S. Greco, A. M. Zoubir, and M. Rangaswamy, "Semiparametric crb and slepian-bangs formulas for complex elliptically symmetric distributions," *IEEE Transactions on Signal Processing*, vol. 67, no. 20, pp. 5352–5364, 2019. III

[13] ——, "Semiparametric inference and lower bounds for real elliptically symmetric distributions," *IEEE Transactions on Signal Processing*, vol. 67, no. 1, pp. 164–177, 2018. III

[14] F. Gini and R. Reggiannini, "On the use of cramer-rao-like bounds in the presence of random nuisance parameters," *IEEE Transactions on Communications*, vol. 48, no. 12, pp. 2120–2126, 2000. IV

[15] S. Fortunati, A. Farina, F. Gini, A. Graziano, M. S. Greco, and S. Giompapa, "Least squares estimation and cramér–rao type lower bounds for relative sensor registration process," *IEEE Transactions on Signal Processing*, vol. 59, no. 3, pp. 1075–1087, 2010. IV

[16] Q. He, R. S. Blum, and A. M. Haimovich, "Noncoherent mimo radar for location and velocity estimation: More antennas means better performance," *IEEE Transactions on Signal Processing*, vol. 58, no. 7, pp. 3661–3680, 2010. IV-A, IV-A

[17] E. Ollila, D. E. Tyler, V. Koivunen, and H. V. Poor, "Complex elliptically symmetric distributions: Survey, new results and applications," *IEEE Transactions on signal processing*, vol. 60, no. 11, pp. 5597–5625, 2012. IV-A

[18] X. Zhang, M. N. El Korso, and M. Pesavento, "Mimo radar performance analysis under k-distributed clutter," in *2014 IEEE International Conference on Acoustics, Speech and Signal Processing (ICASSP)*. IEEE, 2014, pp. 5287–5291. IV-B